Engineering Solid Mechanics 12 (2024) 27-32

Contents lists available at GrowingScience

Engineering Solid Mechanics

homepage: www.GrowingScience.com/esm

Surface morphological characterization of rf-magnetron sputtering developed inconel coated titanium

Kunle Babaremu[a*], Tien-Chen Jen[a], Oluseyi Oladijo[a,b] and Esther Akinlabi[c]

[a]*Mechanical Engineering Department, University of Johannesburg, Auckland, South Africa*
[b]*Department of Chemical, Materials and Metallurgical Engineering, Botswana International University of Science and Technology, Palapye, Botswana*
[c]*Department of Mechanical and Construction Engineering, Faculty of Environment, Northumbria University, Newcastle, United Kingdom*

ARTICLE INFO

Article history:
Received 21 May 2023
Accepted 24 July 2023
Available online
24 July 2023

Keywords:
Magnetron sputtering
Morphology
Surface coatings
Titanium

ABSTRACT

The interconnected usefulness of titanium grade 5 is amplified by the improved mechanical ability and sustainable applications in various industries like the aerospace, medical industry and many more. Despite the profound properties of Ti6Al4V, it is worthy of intellectual study to investigate the possible performance improvement of the material for better operational application. This study adopted the use of RF magnetron sputtering to deposit the target on the substrate material under varying temperatures and deposition power. A total of four samples and control were analyzed for a surface morphological examination and post-sputtering chemical compositional analysis via SEM (scanning electron microscope) and EDX (energy dispersive x-ray analysis). Further investigation on the samples' crystallites was done using XRD (X-ray diffractometer). The SEM images showed low agglomeration and most of the samples were void of pores, cleft and crevices, which implied homogeneous distribution of the target (Inconel thin film) on the titanium substrate. The EDX of the Inconel coated titanium samples revealed elements such as Ti, Si and C, which are beneficial to the properties of the materials. The XRD profiles of the Inconel coated titanium samples disclosed intensities of high peaks, which indicated stability, chemical and microstructural homogeneity of the thin film.

1. Introduction

A grade five titanium is represented with Ti6Al4V which is interpreted as titanium alloy having six percent of aluminium and four percent of vanadium (Babaremu et al., 2022a). It has very impressive mechanical properties like impeccable tensile strength that informs its performance in extreme temperatures. It is heat treatable and has very good weldability characteristics which makes it widely applicable in areas where titanium parts are required for fabrication (Babaremu et al., 2022b). Ti6Al4V is also suitable in saltwater in the event of crack corrosion because it offers very good resistance with further applications in oil and gas offshore extractions. Sputtering is progressively adopted for material surface coatings and development by depositing various targets in the form of the thin film on a base material referred to as substrate (Yuan et al., 2020; Sigmund, 2012). It is referred to as atomic ejection through the bombardment of liquid or solid target particles that are energetic which are mostly ions (Alfonso et al., 2012; Westwood, 1988). Magnetron sputtering could be explained to be the process of the collision that occurs between targets and incident particles. Given that at a low-pressure high-speed sputtering is relatively performed, it is then very important to significantly increase the rate of ionization of the gas (Alexeeva & Fateev, 2016). In the targets, the incident particle undergoes a very complex process of scattering that collides with the atom of the target, and

* Corresponding author.
E-mail addresses: kunle.babaremu@paulesi.org.ng (K. Babaremu)

ISSN 2291-8752 (Online) - ISSN 2291-8744 (Print)

doi: 10.5267/j.esm.2023.7.005

eventually transmit the part of the momentum to the target atom, which in turn collides with other target atoms to form a cascade process (Kashkarov et al., 2020). It is important to note that certain target atoms close to the surface during this cascade gain sufficient momentum for outward motion (Belosludtsev et al., 2020).

Magnetron sputtering technique is used for vacuum coating with high rate operational performance in target depositing of alloys, metals and compounds on a substrate with a millimeter range of thickness. Amongst other utilized techniques for vacuum coating, magnetron sputtering has a better advantage of importance which made it gain increased commercial applications over the years as focus moved to simple decorative coatings from fabrication via microelectronics (Hassan, 2018). Some of the outstanding advantages that magnetron sputtering possesses are ease of automation, heat sensitive substrate coating ability, thin film high adhesion, high thin film purity, high rate of deposition, impressive surface uniformity and many more (Tudose, 2019).

After the description of the non exhaustive advantages and applications of titanium which has immense impact on the surface of interaction during use, there is a need to develop improved processes to upgrade the applicability of the titanium metal in various fields of human endeavor. Feng et al., (2021) emphasized the potentials of the Inconel 625 as a thin film target on any chosen substrates by using magnetron sputtering as the deposition mechanism for improvement of desired properties of the materials. The findings suggested the suitability of the adoption of Inconel for coatings through the sputtering process. Therefore, this study investigated the surface morphological characterization of rf-magnetron sputtering developed Inconel coated titanium.

2. Experimental Procedure

Inconel thin films were prepared through the use of a magnetron sputtering technique on titanium substrate. At a base pressure of 1.13×10^{-5} mbar, the chamber for the sputtering was properly vacuumed. The samples were sputtered at a deposition time of 60 minutes to 90 minutes. Sputtering was relatively achieved at a power rating of 100W to 200W. After the completed process of target thin film layer on the titanium substrate, all the samples were kept in the chamber for sufficient cooling. The cooled samples were taken out of the vacuum and carefully machined into a 10 mm × 10 mm dimension for SEM, EDX and XRD characterization for the surface morphology.

2.1 SEM images and EDX-analysis of samples

Fig. 1 indicates the SEM images and EDX of the titanium control sample. The SEM micrographs at the magnifications of 8000×, 9000× and 1000× were presented. A smooth morphology was observed at 8000× and 9000× magnification. However, at the magnification of 1000× some diagonal clefts were observed on the surface, which could act as sites for the infiltration of contaminants if left unprotected, and this could in turn affects the corrosion and mechanical properties of the sample (Zhang et al., 2021 and Li et al., 2020). The EDX of the sample expectedly indicated that titanium (Ti) was the predominant element in the sample. The other elements in trace quantity are oxygen (O), silicon (Si) and carbon (C).

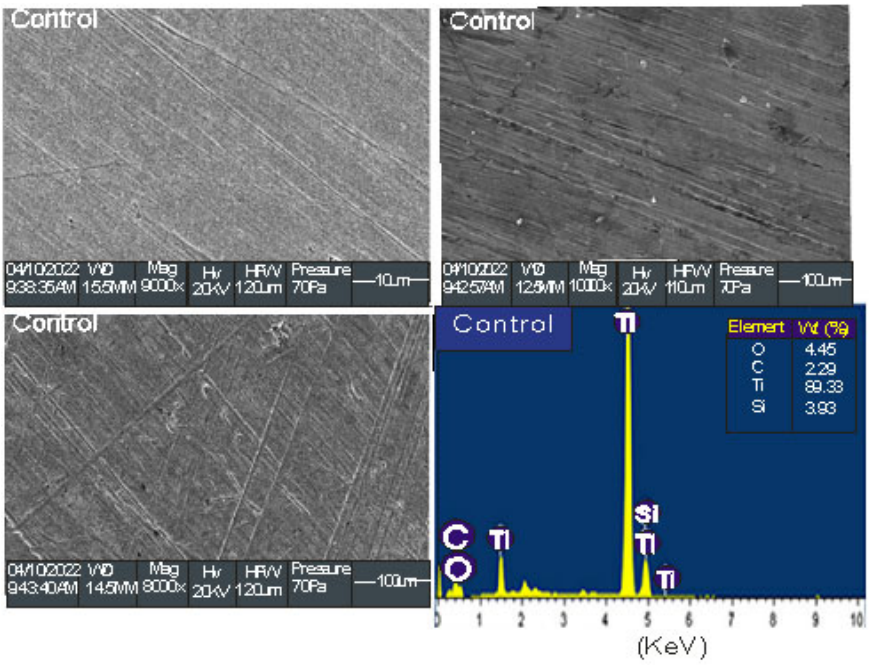

Fig. 1. SEM images and EDX of the titanium control sample

Moreover, Fig. 2 shows the SEM images and EDX of coated samples 1 and 2. Sample 1 was observed to exhibit two unique phases with a distinct surface morphology and redefined microstructure. This indicated that the Inconel inclusion on the surface of the titanium exhibited a grain refining ability, as also reported by Amanov et al., (2015) and Sun et al., (2023). The SEM of sample 2 revealed a more homogeneous phase and puffy morphology, indicating the likely presence of more Inconel film on the titanium surface of the sample. Some degrees of undulations and rifts were also observed on the surface of sample 2, which can act as crevices for the entrance of corrosive substances, hence, leading to material deterioration (Burkert et al., 2018 and Zhang et al., 2018). Moreover, the EDX of samples 1 and 2 exhibited a comparable percentage of titanium (Ti). Some other trace elements observed are carbon (C), oxygen (O) and silicon (Si). While the presence of carbon (C) could enhance the hardness of the materials, the presence of silicon (Si) could be beneficial to the materials' corrosion resistance and mechanical properties (Li et al., 2016; Liu et al., 2018). Silicon (Si) has been employed as an alloying element to enhance high strength and low weight, conductivity, reflectivity, visible light and heat, corrosion resistance and tensile strength (Hemath et al., 2020).

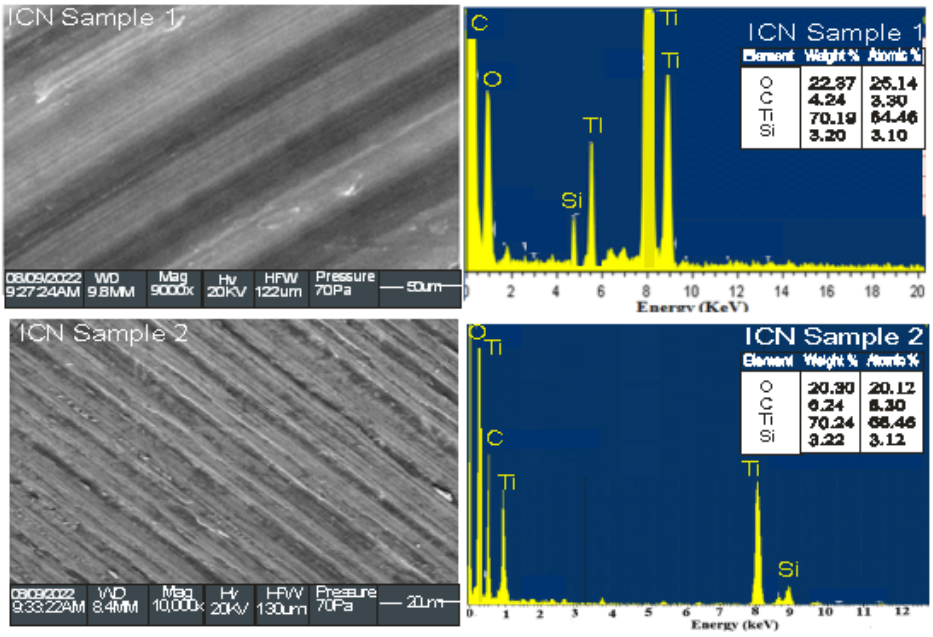

Fig. 2. SEM images and EDX of thin film coated samples 1 and 2

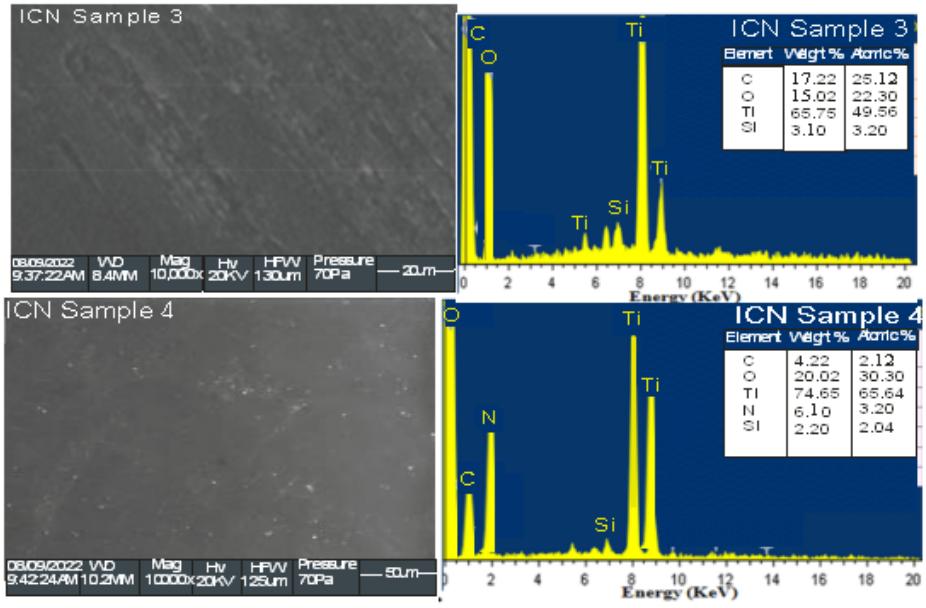

Fig. 3. SEM images and EDX of thin film coated samples 3 and 4

Furthermore, Fig. 3 showed the SEM image and EDX of thin film-coated samples 3 and 4, indicating that the samples exhibited better morphology compared to the other samples. Litter pores were observed on the SEM image of sample 3. Although, the clefts were not as conspicuous as those seen on samples 1, 2 and control. This low level of clefts on the microstructure of sample 3 indicated that the sample could possess superior properties and applicability compared to samples 1, 2 and the control sample (Sevvel et al., 2018). Compared to the entire samples, it is worth noting that sample 4 exhibited the best morphology and most outstandingly refined surface microstructures that are void of particle agglomerations, dimples, pores and clefts. The sample also exhibited smaller grain sizes relative to the other samples. The exceptional morphology of sample 4 revealed that the Inconel thin firm exhibited grain refinement ability as reported by (Sonar et al., 2020 and Jia & Gu, 2014). The EDX of samples 3 and 4 indicated the presence of elements such as carbon (C), Oxygen (O), titanium (Ti) and silicon (Si). A considerable percentage of nitrogen (Ni) was also observed to be present in sample 4.

2.2 X-ray Diffraction (XRD) presentation of crystallites or phases in the samples

Fig. 4 indicated the phases in the control sample (titanium). The highest peak intensity of titanium as a single-phase element was observed at about 1750 a.u (2θ of 29º). This indicated the possibility of titanium being more stable and predominant at this intensity (Ragavendran et al., 2014 and Gong et al., 2017). The other high peak intensities observed are at 1500 a.u (2θ of 24º) and 1000 a.u (2θ of 25º). Some low-intensity crystallites were observed between the 2 theta of 43º and 2θ of 78º. The low intensities indicated crystallites formed from the combination of titanium and other trace elements present. Relative to the control sample, the Inconel coated titanium samples were observed to exhibit lower peak intensities as shown in Fig. 5. This indicated that the Inconel film combined with titanium homogeneously to reduce the dominance of the titanium single element as indicated in Fig. 4. Comparing the entire Inconel coated titanium samples; sample 3 exhibited the highest peak intensity of about 550 a.u at 2 theta of 10º. The other high peak intensities are at 290 a.u (2θ of 22º) and 300 a.u (2θ of 49º).

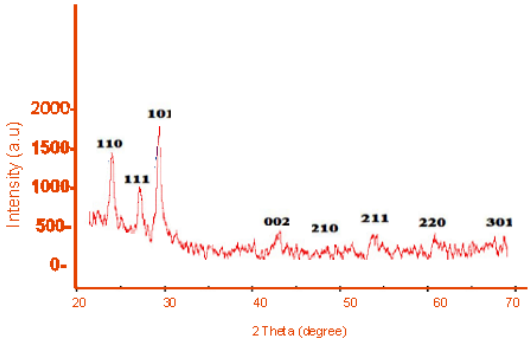

Fig. 4. XRD profile of the titanium control sample

Moreover, sample 4 also exhibited a comparable high peak intensity of about 520 a.u (2θ of 28º), while samples 1 and 2 possessed high peak intensities of 460 a.u (2θ of 10º) and 450 a.u (2θ of 20º), respectively. The peak intensities on the Inconel coated titanium samples showed that the thin film of Inconel was well distributed on the titanium. It also indicated that the coating exhibited chemical and microstructural homogeneity.

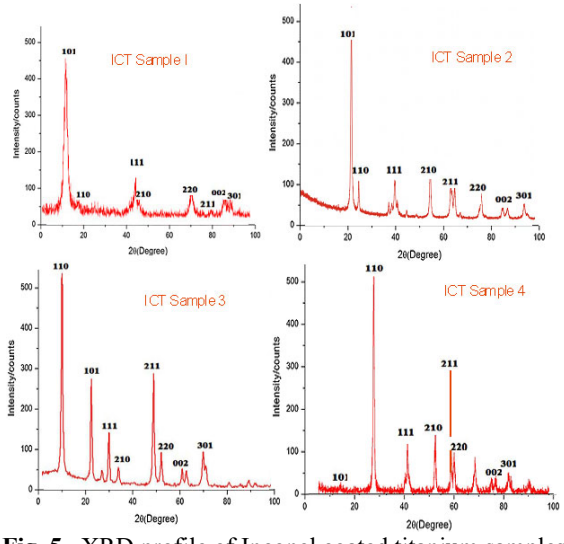

Fig. 5. XRD profile of Inconel coated titanium samples

3. Conclusions

A receptive surface thin film alignment on the various samples was discovered from the analysis which means that they are not susceptible to easy wear impact during operationalization. Morphological behavior of the titanium control sample displayed a level of excellence. The SEM images showed low agglomeration and most of the samples were void of pores, cleft and crevices, which implied homogeneous distribution of the coating. The use of magnetron sputtering was efficient in this study because there are no oxide pores and undulating layers of the Ti structure except for sample 2 with little pores which would affect the adhesion and resistance to scratch failure. Increase in the O element of the titanium sample was as a result of the composition of the Inconel target used for coating the surface as revealed by the EDX analysis. The EDX of the Inconel coated titanium samples revealed elements such as Ti, Si and C, which are beneficial to the properties of the materials. The XRD profiles of the Inconel coated titanium samples disclosed intensities of high peaks, which indicated stability, chemical and microstructural homogeneity of the coating.

Funding: The research received financial support from the University of Johannesburg through the URC.

Ethics approval: N/A

Consent for publication: The authors have decided to publish this article in your prestigious journal.

Conflicts of Interest: The authors of the article titled “Evaluation of Microstructure, Corrosion and Wear Characteristics of TI6Al4V Sputtered Inconel 625 Film” do not have any conflict of interest regarding this manuscript.

Author contributions KB: article writing, OO, TC and EA: supervision, All authors reviewed the article.

Availability of data and materials: Corresponding author will make it available on valid request.

References

Alexeeva, O. K., & Fateev, V. N. (2016). Application of the magnetron sputtering for nanostructured electrocatalysts synthesis. *International journal of hydrogen energy*, *41*(5), 3373-3386. doi: 10.1016/j.ijhydene.2015.12.147.

Alfonso, E., Olaya, J., & Cubillos, G. (2012). Thin film growth through sputtering technique and its applications. *Crystallization-Science and technology*, *23*, 11-12. doi: 10.5772/35844.

Amanov, A., Pyun, Y. S., Kim, J. H., Suh, C. M., Cho, I. S., Kim, H. D., ... & Khan, M. K. (2015). Ultrasonic fatigue performance of high temperature structural material Inconel 718 alloys at high temperature after UNSM treatment. *Fatigue & Fracture of Engineering Materials & Structures*, *38*(11), 1266-1273, doi.org/10.1111/ffe.12330.

Babaremu, K. O., Jen, T. C., Oladijo, P. O., & Akinlabi, E. T. (2022). Mechanical, Corrosion Resistance Properties and Various Applications of Titanium and Its Alloys: A Review. *Revue des Composites et des Matériaux Avancés*, *32*(1).

Babaremu, K., Jen, T. C., Oladijo, P., & Akinlabi, E. (2022). A systematic review of the effects of deposition parameters on the properties of Inconel thin films. *The International Journal of Advanced Manufacturing Technology*, 1-21.

Belosludtsev, A., Vlček, J., Houška, J., Haviar, S., and Čerstvý, R. “Tunable composition and properties of Al-O-N films prepared by reactive deep oscillation magnetron sputtering,” *Surface and Coatings Technology*, vol. 392, no. January, p. 125716, 2020, doi: 10.1016/j.surfcoat.2020.125716.

Burkert, A., Müller, T., Lehmann, J., & Mietz, J. (2018). Long-term corrosion behaviour of stainless steels in marine atmosphere. *Materials and Corrosion*, *69*(1), 20-28, doi.org/10.1002/maco.201709636.

Feng, J., Yuan, G., Mao, L., Leão, J. B., Bedell, R., Ramic, K., ... & Liu, L. (2021). Probing layered structure of Inconel 625 coatings prepared by magnetron sputtering. *Surface and Coatings Technology*, *405*, 126545.

Gong, F., Zhang, J., Ding, L., Yang, Z., & Liu, X. (2017). Mussel-inspired coating of energetic crystals: A compact core–shell structure with highly enhanced thermal stability. *Chemical Engineering Journal*, *309*, 140-150, doi.org/10.1016/j.cej.2016.10.020.

Hassan, M. M. (2018). *Antimicrobial Coatings for Textiles. Handbook of Antimicrobial Coatings, 321–355.* doi:10.1016/b978-0-12-811982-2.00016-0

Hemath, M., Mavinkere Rangappa, S., Kushvaha, V., Dhakal, H. N., & Siengchin, S. (2020). A comprehensive review on mechanical, electromagnetic radiation shielding, and thermal conductivity of fibers/inorganic fillers reinforced hybrid polymer composites. *Polymer Composites*, *41*(10), 3940-3965, https://doi.org/10.1002/pc.25703.

Jia, Q., & Gu, D. (2014). Selective laser melting additive manufacturing of Inconel 718 superalloy parts: Densification, microstructure and properties. *Journal of Alloys and Compounds*, *585*, 713-721, doi.org/10.1016/j.jallcom.2013.09.171.

Kashkarov, E. B., Sidelev, D. V., Rombaeva, M., Syrtanov, M. S., & Bleykher, G. A. (2020). Chromium coatings deposited by cooled and hot target magnetron sputtering for accident tolerant nuclear fuel claddings. *Surface and Coatings Technology*, *389*, 125618. doi: 10.1016/j.surfcoat.2020.125618.

Kumar, P., Shahzad, F., Yu, S., Hong, S. M., Kim, Y. H., & Koo, C. M. (2015). Large-area reduced graphene oxide thin film with excellent thermal conductivity and electromagnetic interference shielding effectiveness. *Carbon*, *94*, 494-500, https://doi.org/10.1016/j.carbon.2015.07.032.

Li, B. Q., Xie, R. Z., & Lu, X. (2020). Microstructure, mechanical property and corrosion behavior of porous Ti–Ta–Nb–Zr. *Bioactive Materials*, *5*(3), 564-568, doi.org/10.1016/j.bioactmat.2020.04.014.

Li, W., Li, S., Liu, J., Zhang, A., Zhou, Y., Wei, Q., ... & Shi, Y. (2016). Effect of heat treatment on AlSi10Mg alloy fabricated by selective laser melting: Microstructure evolution, mechanical properties and fracture mechanism. *Materials Science and Engineering: A*, *663*, 116-125, doi.org/10.1016/j.msea.2016.03.088.

Liu, Y. J., Liu, Z., Jiang, Y., Wang, G. W., Yang, Y., & Zhang, L. C. (2018). Gradient in microstructure and mechanical property of selective laser melted AlSi10Mg. *Journal of Alloys and Compounds*, *735*, 1414-1421, doi.org/10.1016/j.jallcom.2017.11.020.

Ragavendran, K. R., Xia, H., Yang, G., Vasudevan, D., Emmanuel, B., Sherwood, D., & Arof, A. K. (2014). On the theory of high rate capability of $LiMn_2O_4$ with some preferred orientations: insights from the crystal shape algorithm. *Physical chemistry chemical physics*, *16*(6), 2553-2560, doi.org/10.1039/C3CP54439G.

Sevvel, P., Satheesh, C., & Jaiganesh, V. (2018). Influence of tool rotational speed on microstructural characteristics of dissimilar Mg alloys during friction stir welding. *Transactions of the Canadian Society for Mechanical Engineering*, *43*(1), 132-141, doi.org/10.1139/tcsme-2018-003.

Sigmund, P. (2012). Recollections of fifty years with sputtering. *Thin Solid Films*, *520*(19), 6031-6049. doi: 10.1016/j.tsf.2012.06.003.

Sonar, T., Balasubramanian, V., Malarvizhi, S., Nagar, A., Venkateswaran, T., & Sivakumar, D. (2020). Microstructural characteristics and tensile properties of gas tungsten constricted arc (GTCA) welded Inconel 718 superalloy sheets for aeroengine components. *Materials Testing*, *62*(11), 1099-1108, doi.org/10.3139/120.111576.

Sun, P., Wang, D., Song, W., Tang, C., Yang, J., Xu, Z., ... & Zeng, X. (2023). Influence of W content on microstructure and corrosion behavior of laser cladded Inconel 718 coating. *Surface and Coatings Technology*, *452*, 129079, doi.org/10.1016/j.surfcoat.2022.129079.

Tudose, I. V., Comanescu, F., Pascariu, P., Bucur, S., Rusen, L., Iacomi, F., … Suchea, M. P. (2019). *Chemical and physical methods for multifunctional nanostructured interface fabrication. Functional Nanostructured Interfaces for Environmental and Biomedical Applications, 15–26.* doi:10.1016/b978-0-12-814401-5.00002-5

Westwood, W. D. (1988). Sputter Deposition Processes. *MRS Bulletin*, *13*(12), 46–51, 1988, doi: 10.1557/S0883769400063697.

Yuan, X., Liang, S., Ke, H., Wei, Q., Huang, Z., & Chen, D. (2020). Photocatalytic property of polyester fabrics coated with Ag/TiO2 composite films by magnetron sputtering. *Vacuum*, *172*, 109103, 2020, doi: 10.1016/j.vacuum.2019.109103.

Zhang, B., Wang, J., & Yan, F. (2018). Load-dependent tribocorrosion behaviour of nickel-aluminium bronze in artificial seawater. *Corrosion Science*, *131*, 252-263, https://doi.org/10.1016/j.corsci.2017.11.028.

Zhang, Q., Li, Q., & Chen, X. (2021). The effects of Sn content on the corrosion behavior and mechanical properties of Mg–5Gd–3Y–x Sn–0.5 Zr alloys. *RSC advances*, *11*(3), 1332-1342, doi.10.1039/dora08986a.